Rational design of azepane-glycoside antibiotics targeting the bacterial ribosome

Sofia Barluenga,[a,†] Klaus B. Simonsen,[a] Ethel S. Littlefield,[a] Benjamin K. Ayida,[a]
Dionisios Vourloumis,[a] Geoffrey C. Winters,[a] Masayuki Takahashi,[a] Sarah Shandrick,[b]
Qiang Zhao,[b] Qing Han[b] and Thomas Hermann[b,*]

[a]*Department of Medicinal Chemistry, Anadys Pharmaceuticals, Inc., 9050 Camino Santa Fe, San Diego, CA 92121, USA*
[b]*Departments of RNA Biochemistry and Structural Chemistry, Anadys Pharmaceuticals, Inc., 9050 Camino Santa Fe,
San Diego, CA 92121, USA*

Abstract—RNA recognition by natural aminoglycoside antibiotics depends on the 2-deoxystreptamine (2-DOS) scaffold which participates in specific hydrogen bonds with the ribosomal decoding-site target. Three-dimensional structure information has been used for the design of azepane-monoglycosides, building blocks for novel antibiotics in which 2-DOS is replaced by a heterocyclic scaffold. Azepane-glycosides showed target binding and translation inhibition in the low micromolar range and inhibited growth of *Staphylococcus aureus*, including aminoglycoside-resistant strains.
© 2003 Elsevier Ltd. All rights reserved.

1. Introduction

The bacterial ribosome is a key target for many antibiotics,[1] among them natural aminoglycosides such as paromomycin, neomycin B, and neamine (Fig. 1a). Aminoglycoside antibiotics interact specifically with the decoding-site ribosomal RNA (rRNA) (Fig. 1b)[2–4] and disrupt functional protein synthesis by interfering with mRNA-decoding fidelity.[5–7] Upon binding, aminoglycosides displace two key adenine residues from the deep groove of the decoding-site rRNA. The ensuing conformational change in the adenines, which are involved in contacts to the mRNA–tRNA hybrid, leads to reduced discrimination against noncognate tRNAs and therefore decreased translational accuracy.[6,7] The efficacy of aminoglycosides as antibiotics is compromised by undesirable pharmacological profiles and resistance development.[8,9] Their capacity to bind with high affinity to the bacterial decoding site and several other RNA targets,[10] however, renders them a lead paradigm in RNA molecular recognition.[11–14] Therefore, aminogly-

cosides and fragments thereof constitute ideal starting points for the design and synthesis of novel RNA binders and antibiotics. In previous approaches towards novel aminoglycosides, the 2-deoxystreptamine (2-DOS)[15,16] and glucosamine fragments[17–19] (Fig. 1a) have been derivatized as individual moieties and in context of the neamine[20–23] and paromamine[24,25] scaffolds. Rational design of RNA-targeted novel aminoglycosides is now feasible based on three-dimensional structures, which were recently determined for complexes of the bacterial decoding-site RNA[26–29] and whole ribosomal subunits.[7,30] Synthetic aminoglycosides may achieve binding affinity and specificity for the decoding-site RNA target, and antibacterial potency comparable to the natural antibiotics, however, potentially without being compromised by resistance mechanisms specific for the natural products.

In our efforts to develop novel antibiotics, we have systematically studied aminoglycoside mimetics targeted at the bacterial decoding-site RNA.[16,18,19,25] Here, we describe the design and synthesis of a series of azepane–glycosides, in which a substituted heterocycle has been introduced to mimic the unique spatial arrangement of key functional groups in 2-DOS (Fig. 1c–e), a universally conserved scaffold of natural aminoglycoside antibiotics. Moreover, we report the in vitro and biolo-
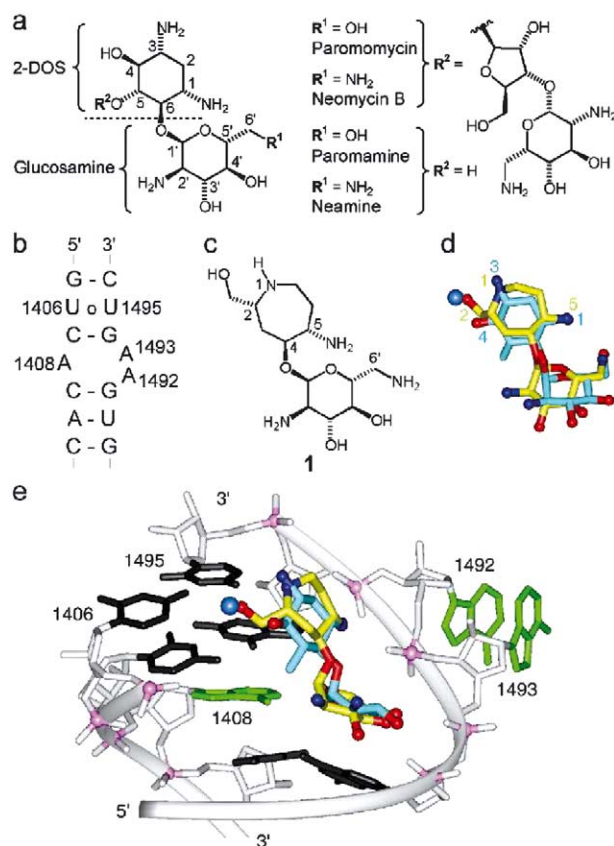
Figure 1. (a) Natural aminoglycoside antibiotics such as paromomycin and neomycin B are derived from paromamine and neamine, which share the 2-deoxystreptamine (2-DOS) and glucosamine cores, both of which are involved in RNA molecular-recognition. (b) Secondary structure of the bacterial decoding-site RNA. (c) Design concept of an azepane-glycoside ligand, **1**, for the decoding-site RNA, derived from coupling of 6-aminoglucosamine with a 5-aminoazepane scaffold as 2-DOS mimetic. (d) Energy-minimized solution conformation of the designed azepane-glycoside **1** (yellow) superimposed on paromamine (blue). Note that the exocyclic 3-amino functionality of paromamine is replaced by the endocyclic secondary amine in the azepane ring, and the 2-hydroxymethyl substituent in the azepane derivative coincides with a water molecule hydrogen-bonded to the 4-hydroxy group of paromamine in the RNA complex. (e) Model of the azepane–glycoside **1** (yellow) docked to the three-dimensional structure[7,30] of the bacterial decoding-site RNA in complex with paromomycin (blue; only paromamine core shown). RNA bases are in dark, sugar phosphate backbone in light grey with phosphate groups emphasized in magenta. A water molecule participating in the non-Watson–Crick U1406/U1495 base pair[26,27] and interacting with a 2-DOS hydroxy group is shown as blue sphere. The flipped-out adenine residues 1492 and 1493, and the unpaired adenine 1408 are shown in green.

gical testing of the synthetic azepane–glycosides for their inhibitory potency against bacterial protein synthesis and cell growth.

2. Design of the azepane-glycosides

The azepane scaffold as a mimetic of 2-DOS was designed by molecular modeling (see Experimental) based on the crystal structure[7,30] of paromomycin complexed with the bacterial decoding site (Fig. 1). The design of the seven-membered heterocycle in **1** (Fig. 1c) was aimed at achieving the distinct spatial arrangement of the 2-DOS amino groups, one of which was incor-

porated into the azepane ring, thereby modulating the amine basicity. Conformational analysis showed that the azepane ring in **1** adopts preferentially a conformation that projects the amino groups at similar vectors as in 2-DOS while optimizing the potential interaction surface of the cyclic system (Fig. 1d). A hydroxy group at the 4-position, and in *anti*-configuration relative to the adjacent exocyclic amino functionality, provided a handle for the attachment of a glucosamine sugar. A hydroxymethyl group next to the endocyclic secondary amine could potentially dock into the binding site of a structurally conserved water molecule at the deep-groove edge of the U1406/U1495 base pair (Fig. 1e). The hydroxymethyl functionality provided also an attachment site for further substitutions of the azepane-glycoside core scaffold.

3. Synthesis

The key step for the synthesis of the 4,5-disubstituted azepanes relied on a ring-closing metathesis reaction[31–33] which gave access to the seven-membered ring containing a double bond as a handle for further derivatization. The development of improved catalysts[34] which tolerate a broad range of functionalities within the molecule, has rendered olefin metathesis the reaction of choice for the construction of medium-sized rings.[35,36] We planned the preparation of the 4-hydroxy-5-azido-azepane **10** from alkene **5** by epoxidation followed by azide opening of the intermediate **7**. Alkene **5** would arise in the forward direction by metathesis of the olefinic groups in intermediate **4**. It was anticipated that the rigid nature of the cyclic carbamate in **4** would accelerate the metathesis reaction by providing a favorable pre-orientation of the olefin moieties.

Synthesis of the glycosylic acceptors **8–11** commenced with the preparation and functionalization of alkene **5** as outlined in Figure 2. The precursor for the metathesis, **4**, was prepared in five steps from L-allylglycine (**2**). Esterification of **2** followed by protection of the amine and subsequent ester reduction produced a mixture of the cyclic carbamate **3** and the expected primary alcohol, which was completely converted to **3** upon base treatment. Alkylation of **3** with 4-bromo-1-butene furnished **4** in good overall yields. DMF was essential as a cosolvent in this alkylation step to prevent decomposition of 4-bromo-1-butene during the prolonged reaction time necessary for completion. Exposure of **4** to 1st generation Grubbs catalyst[31,32] afforded **5** as the only detectable product in 85% yield. Complete consumption of **4** to produce **5** was observed within 10 min, even at relative high substrate concentration (0.2 M), supporting the importance of pre-orientation of the reacting olefins in the metathesis step. Epoxidation of **5** produced a 2:1 mixture of diastereomeric epoxides, which were separated by column chromatography on deactivated silica gel, to avoid decomposition during the purification, to afford the pure isomers (*syn*-**6**, and *anti*-**7**) in acceptable yields. Azide opening of the epoxide isomers **6** and **7** produced the acceptors **8–11** in overall good yields. The *anti* relationship of epoxide **7** and the configuration of azido alcohol **9** were unequivocally
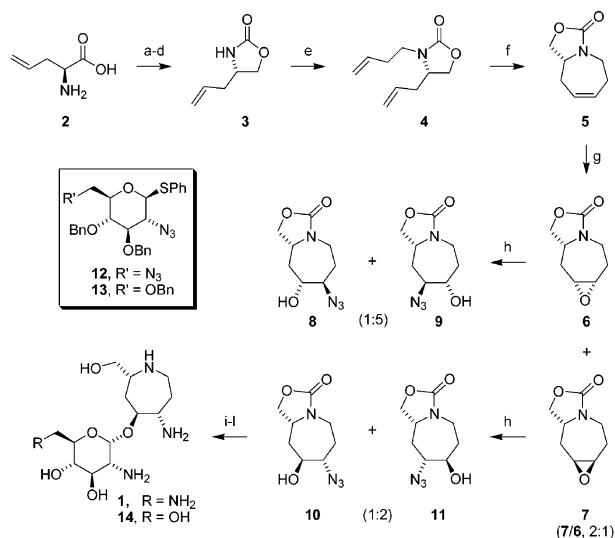
Figure 2. Synthesis of the active azepane-glycoside isomers; Reagents and solvents: (a) SOCl₂, MeOH; (b) CbzCl, NaHCO₃, H₂O/dioxane; (c) LiAlH₄, THF; (d) NaH, THF; (e) 4-bromo-1-butene, Cs₂CO₃, DMF/THF; (f) Grubbs catalyst, CH₂Cl₂; (g) 1,1,1-trifluoroacetone, oxone; (h) NaN₃, EtOH/H₂O; (i) **12** or **13**, NIS, TfOH; (j) KOH, EtOH; (k) Me₃P, THF, H₂O; (l) Pd(OH)₂, H₂, AcOH. Ph, phenyl; Bn, benzyl; Cbz, benzyloxycarbonyl; THF, tetrahydrofuran; DMF, *N,N*-dimethylformamide; Grubbs catalyst, benzylidine-bis(tricyclohexyl-phosphine)dichlororuthenium; oxone, potassium peroxymonosulfate; NIS, *N*-iodosuccinimide; TfOH, trifluorosulfonic acid.

Figure 3. Synthesis of azepane-glycoside derivatives of **1**; Reagents and solvents: (a) Me₃P, THF; (b) Pd(OH)₂, H₂, AcOH; (c) KOH, EtOH; (d) HCHO, NaCNBH₃, ZnCl₂, MeOH; (e) Me₃P, THF; (f) Pd(OH)₂, H₂, AcOH; (g) Me₃P, THF; (h) CbzCl, NaHCO₃, H₂O/dioxane; (i) **19→20**: (i) MsCl, pyridine, (ii) LiCl, DMF, (iii) Pd(OH)₂, H₂, AcOH; **19→21**: (i) DAST, CH₂Cl₂, (ii) Pd(OH)₂, H₂, AcOH; **19→22**: (i) MsCl, pyridine, (ii) NaN₃, DMF, (iii) Pd(OH)₂, H₂, AcOH, (iv) Me₃P, THF. Ms, methanesulfonyl; DAST, (diethylamido)sulfur trifluoride.
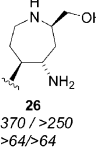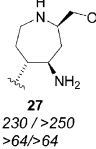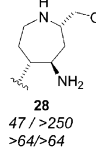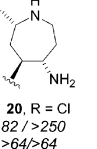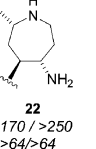
4. Biological activity and structure–activity relationship

The synthesized azepane-glycosides were tested for their activity as inhibitors of bacterial in vitro translation and growth, as well as for their toxicity against eukaryotic cells, and for binding to the bacterial decoding-site RNA target (see Experimental).

The azepane-glycoside **1** and its diastereomer **23** were inhibitors of bacterial in vitro translation at low micromolar concentrations (Table 1 and Fig. 4). While both compounds showed antibacterial activity against the Gram-positive *Staphylococcus aureus*, the isomer **23** was more potent (MIC = 64 and 32 μg/mL for **1** and **23**, respectively). Importantly, both azepane-glycosides, **1** and **23**, retained their antibacterial potency against aminoglycoside-resistant *S. aureus* (MIC = 64 and 32 μg/mL for **1** and **23**, respectively, against multi-drug-resistant BAA40 and BAA44 strains). Neither **1** or **23** inhibited growth of the Gram-negative *Escherichia coli* at 64 μg/mL or interfered with proliferation of eukaryotic cells up to the highest concentration tested (150 μg/mL), corresponding to a CC₅₀ > 320 μM.

Modeling studies suggested that although the azepane scaffold adopts distinct conformations in the diastereomers **1** and **23**, the latter isomer could be docked to the decoding-site target in a similar fashion as the originally designed compound **1**. The diastereomer **24**, which contains the enantiomeric azepane scaffold of **1**, showed no significant potency against bacterial translation or growth, in line with its weak affinity for the decoding-site RNA. The affinity of **1** and **23** for binding to the decoding site RNA (Fig. 4) was at similar levels in the low micromolar range, supporting the proposed mode of action for these translation inhibitors as ligands of the bacterial rRNA target.

determined by single crystal X-ray structure analysis (data not shown).

Synthesis of the final products is outlined exemplarily for compounds **1** and **14** (Fig. 2). Glycosylation of the inseparable 1:2 mixture of **10** and **11** with donors **12** or **13**[18,19,21] provided the α-pseudo-disaccharides as the only detectable anomers, which were separated by column chromatography to afford the pure regioisomers. A three-step deprotection protocol completed the synthesis of **1** and **14**. Specifically, the carbamate functionality was base-cleaved to produce the hydroxy-methyl azido-azepane which was reduced to the corresponding amine (see compound **29**, Table 1) and finally hydrogenolyzed to furnish **1** and **14** in overall good yields. The remaining diastereomers **23–28** were synthesized following the same protocol starting either from pure L-, D-, or racemic allylglycine.

The synthesis of derivatives of **1** (Fig. 3) used intermediate **15** which was obtained by coupling of **10** and **12**. Carbamate **16** was prepared from **15** by a two-step deprotection sequence. Carbamate cleavage of **15** produced the corresponding hydroxymethyl analogue **17**, which was converted to the *N*-methyl analogue **18** by reductive amination followed by a two-step deprotection protocol. Compound **17** was converted to **19** in two steps, which was further reacted with DAST to produce **21** after deprotection. Mesylation of **19** followed by chloride or azide displacement gave rise, after deprotection, to **20** and **22,** respectively.
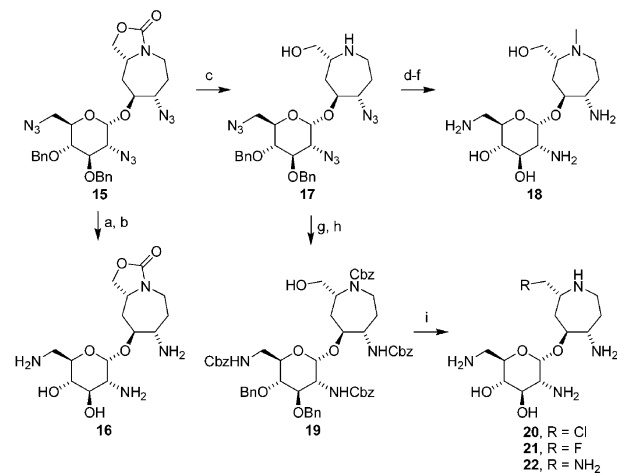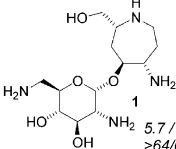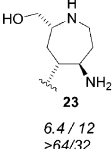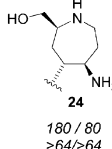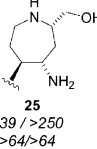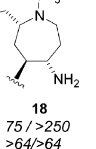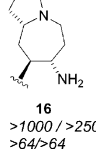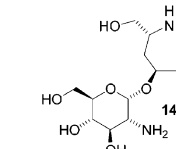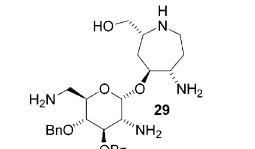
Table 1. Structure–activity relationships for synthetic azepane-glycosides[a]

Structure Compd #	IVT IC$_{50}$ [μM]/RNA IC$_{50}$ [μM][b] MIC [μg/mL] (*E. coli*/*S. aureus*)

1 5.7 / 11 >64/64
23 6.4 / 12 >64/32
24 180 / 80 >64/>64

25 39 / >250 >64/>64
26 370 / >250 >64/>64
27 230 / >250 >64/>64
28 47 / >250 >64/>64

20, R = Cl 82 / >250 >64/>64
21, R = F 36 / >250 >64/>64
22 170 / >250 >64/>64
18 75 / >250 >64/>64
16 >1000 / >250 >64/>64

14 110 / >250 >64/>64
29 >1000 / >250 >64/>64

[a] The diastereomers **23** and **24**, regioisomers **25–28**, and derivatives **16**, **18**, and **20–22** contained the same amino-glucosamine moiety shown for the designed isomer **1**.
[b] IC$_{50}$ values are means of six replicate experiments for each compound (±10%).

Exchange of the 2-hydroxymethyl group in **1** to a halogen or amino group in the azepane-glycoside, like in the derivatives **20**, **21**, and **22**, or methylation of N1 in **18**, reduced the activity of these compounds as translation inhibitors by more than 10-fold, eventually leading to loss of antibacterial potency. None of these derivatives retained binding to the decoding-site RNA, indicating the involvement of both the 2-hydroxymethyl and N1 amino groups in target recognition. According to the design of the azepane scaffold (Fig. 1c–e), the amino hydrogen atom of N1 is required for a hydrogen-bonding interaction with the decoding-site RNA. The residual inhibitory activity of **18**, **20**, and **21** in the translation assay might be due to nonspecific action on a ribosomal target other than the decoding site. The carbamate derivative **16** was completely inactive in both the bacterial translation and growth inhibition assays, further supporting the importance of the free hydroxymethyl and the amine functionality for interactions with the target.

Among the regioisomers (**25–28**) of **1**, the azepane–glycosides **25** and **28** showed moderate inhibition of bacterial
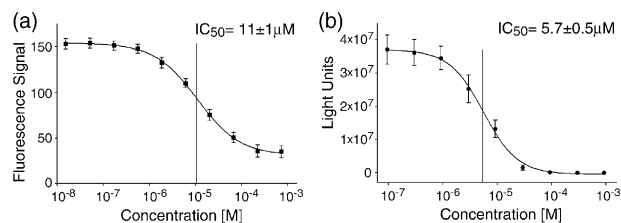

Figure 4. Dose–response curves and IC$_{50}$ values calculated thereof for the azepane-glycoside **1** showing (**a**) binding of the ligand to the bacterial decoding-site RNA in a fluorescence assay, and (**b**) inhibition of bacterial in vitro translation by the compound. The binding curve was obtained as an average of two titrations and fitted to a single-site model, resulting in a Hill-coefficient of 0.95. The translation inhibition curve was calculated by averaging over six independent dose–response experiments. Error bars indicate ±1σ.

translation, however, likely due to interference with a ribosomal target distinct from the decoding site, as binding to the latter target was not detectable. None of the regioisomers **25–28** inhibited bacterial growth at concentrations ≤64 μg/mL. Modeling studies indicated that, in such regioisomers, the hydroxymethyl substituent interferes sterically with the docking of the 5-amino-azepane scaffold to the decoding-site RNA.

Change of the amino sugar moiety in **1** to the hydroxy derivative in **14** resulted in a more than 10-fold loss of activity in the translation assay, comparable to the difference in potency between the natural aminoglycosides neamine and paromamine,[4,18] the corresponding 2-DOS derivatives of these sugars. Consequently, the compound **14** did not inhibit bacterial growth. The importance of the sugar moiety for RNA target recognition by the azepane-glycosides was further underlined by the finding that the benzylated derivative **29** was completely inactive in both the translation and growth inhibition assays.

5. Conclusion

A rational ligand discovery approach has been used to design and synthesize novel azepane-glycosides that bind to the bacterial decoding-site RNA, and thereby inhibit bacterial translation in vitro. Two of the designed ligands showed moderate antibacterial activity against *S. aureus* and retained this activity against aminoglycoside-resistant strains. A small number of isomers and derivatives has been synthesized and tested, revealing a preliminary structure–activity relationship of the azepane-glycosides and underlining the importance of stereochemical design for antibiotic activity with only the initially designed stereoisomers as inhibitors of in vitro translation and bacterial growth. The activity of the azepane-glycosides against aminoglycoside-resistant strains demonstrates that designed scaffolds can be used to mimic the biological activity of natural antibiotics, while being sufficiently distinct from the natural products to escape some resistance mechanisms. The result substantiates the importance of the bacterial decoding site as a valuable target for future development of novel antibiotics that may share many of the positive characteristics of the aminoglycoside antibacterials, such as

potency and bacteriocidality, without being compromised by the widespread pathogen resistance against these drugs.

6. Experimental

6.1. Molecular modelling

Compound design and docking was performed using atom coordinates of the 30S ribosomal subunit–aminoglycoside complexes[7,30] and crystal structures of synthetic RNA constructs containing the bacterial decoding-site internal loop (Q. Zhao, T. Hermann, unpublished results). Preferred conformations of the azepane heterocycle and the azepane-glycosides were explored by molecular dynamics simulations and energy minimization following established protocols.[37,38]

6.2. Determination of RNA target binding

Compounds were tested for binding to the decoding-site target using an RNA fluorescence assay which determines the binding affinity of a ligand based on its ability to flip out the flexible adenines A1492 and A1493 in a model oligonucleotide (compare Fig. 1). The assay thus returns a true measure of the potency of a compound to bind specifically to the decoding-site internal loop and to induce a conformational response comparable to that triggered by natural aminoglycoside antibiotics. Complete experimental details of the assay will be reported separately.

6.3. Determination of translation inhibition

To assess potency of compounds as translation inhibitors, a coupled in vitro transcription–translation assay was carried out as previously described.[16,25]

6.4. Determination of bacterial growth inhibition

The antibacterial activity of compounds was evaluated for *Escherichia coli* (strain ATCC-25922) and *Staphylococcus aureus* (ATCC-25923) by determining the minimal inhibitory concentration (MIC).[39] Two-fold dilutions ranging from 64 to 0.03 µg/mL were tested in triplicate. The MIC was determined as the lowest compound concentration that prevented cell growth after 18 h of incubation at 37 °C. The same protocol was used to test aminoglycoside-resistant pathogens, including methicillin-resistant *Staphylococcus aureus* (ATCC strain numbers BAA40 and BAA44, respectively, which are Portuguese and Iberian clones of MRSA)[39–41] which carry multi-drug-resistance against decoding-site binding aminoglycosides, such as gentamicin, neomycin, and other antibiotics, including macrolides, ampicillin, erythromycin, penicillin, tetracycline, methicillin, oxacillin, and spectinomycin.

6.5. Determination of cytotoxicity

The eukaryotic cytotoxicity of compounds was assessed in a standard proliferation assay measuring the mitochondrial reduction of XTT into an orange formazan dye by T-cells.[42] After cells were incubated with series of compound concentrations for 72 h, XTT solution was added and fluorescence read at 450 nm and 650 nm. The 50% cytotoxic concentration (CC_{50}) was defined as the compound concentrations required to reduce by 50% the number of viable cells.

References and notes

1. Gale, E. F.; Cundliffe, E.; Renolds, P. E.; Richmond, M. H.; Waring, M. J. *The Molecular Basis of Antibiotic Action*; John Wiley and Sons: London, 1981.
2. Moazed, D.; Noller, H. F. *Nature* **1987**, *327*, 389.
3. Purohit, P.; Stern, S. *Nature* **1994**, *370*, 659.
4. Wong, C.-H.; Hendrix, M.; Priestley, E. S.; Greenberg, W. A. *Chem. Biol.* **1998**, *5*, 397.
5. Ramakrishnan, V. *Cell* **2002**, *108*, 557.
6. Fourmy, D.; Yoshizawa, S.; Puglisi, J. D. *J. Mol. Biol.* **1998**, *277*, 333.
7. Ogle, J. M.; Brodersen, D. E.; Clemons, W. M.; Tarry, M. J.; Carter, A. P.; Ramakrishnan, V. *Science* **2001**, *292*, 897.
8. Wright, G. D.; Berghuis, A. M.; Mobashery, S. In *Resolving the Antibiotic Paradox: Progress in Understanding Drug Resistance and Development of New Antibiotics*; Rosen, B. P., Mobashery, S., Eds.; Plenum: New York, 1998; pp 27–69.
9. Kotra, L. P.; Haddad, J.; Mobashery, S. *Antimicrob. Agents Chemother.* **2000**, *44*, 3249.
10. Schroeder, R.; Waldsich, C.; Wank, H. *EMBO J.* **2000**, *19*, 1.
11. Tor, Y.; Hermann, T.; Westhof, E. *Chem. Biol.* **1998**, *5*, R277.
12. Hermann, T.; Westhof, E. *Biopolymers Nucleic Acid Sciences* **1999**, *48*, 155.
13. Hermann, T. *Angew. Chem., Int. Ed. Engl.* **2000**, *39*, 1890.
14. Hermann, T. *Biochimie* **2002**, *84*, 865.
15. Ding, Y.; Hofstadler, S. A.; Swayze, E. E.; Griffey, R. H. *Org. Lett.* **2001**, *3*, 1621.
16. Vourloumis, D.; Takahashi, M.; Winters, G. C.; Simonsen, K. B.; Ayida, B. K.; Barluenga, S.; Qamar, S.; Shandrick, S.; Zhao, Q.; Hermann, T. *Bioorg. Med. Chem. Lett.* **2002**, *12*, 3367.
17. Wong, C.-H.; Hendrix, M.; Manning, D. D.; Rosenbohm, C.; Greenberg, W. A. *J. Am. Chem. Soc.* **1998**, *120*, 8319.
18. Vourloumis, D.; Winters, G. C.; Takahashi, M.; Simonsen, K. B.; Ayida, B. K.; Shandrick, S.; Zhao, Q.; Hermann, T. *ChemBioChem* **2003**, *4*, 879.
19. Simonsen, K. B.; Ayida, B. K.; Vourloumis, D.; Winters, G. C.; Takahashi, M.; Shandrick, S.; Zhao, Q.; Hermann, T. *ChemBioChem* **2003**, *4*, 886.
20. Alper, P.; Hendrix, M.; Sears, P.; Wong, C.-H. *J. Am. Chem. Soc.* **1998**, *120*, 1965.
21. Greenberg, W. A.; Priestley, E. S.; Sears, P. S.; Alper, P. B.; Rosenbohm, C.; Hendrix, M.; Hung, S.-C.; Wong, C.-H. *J. Am. Chem. Soc.* **1999**, *121*, 6527.

22. Nunns, C. L.; Spence, L. A.; Slater, M. J.; Berrisford, D. J. *Tetrahedron Lett.* **1999**, *40*, 9341.
23. Haddad, J.; Kotra, L.; Llano-Sotelo, P. B.; Kim, C.; Azucena, E. F.; Liu, M.; Vakulenko, S. B.; Chow, C. S.; Mobashery, S. *J. Am. Chem. Soc.* **2002**, *124*, 3229.
24. Hanessian, S.; Tremblay, M.; Kornienko, A.; Moitessier, N. *Tetrahedron* **2001**, *57*, 3255.
25. Simonsen, K. B.; Ayida, B. K.; Vourloumis, D.; Takahashi, M.; Winters, G. C.; Barluenga, S.; Qamar, S.; Shandrick, S.; Zhao, Q.; Hermann, T. *ChemBioChem.* **2002**, *3*, 1223.
26. Vicens, Q.; Westhof, E. *Structure* **2001**, *9*, 647.
27. Vicens, Q.; Westhof, E. *Chem. Biol.* **2002**, *9*, 747.
28. Fourmy, D.; Recht, M. I.; Blanchard, S. C.; Puglisi, J. D. *Science* **1996**, *274*, 1367.
29. Russell, R. J. M.; Murray, J. B.; Lentzen, G.; Haddad, J.; Mobashery, S. *J. Am. Chem. Soc.* **2003**, *125*, 3410.
30. Carter, A. P.; Clemons, W. M.; Brodersen, D. E.; Morgan-Warren, R. J.; Wimberly, B. T.; Ramakrishnan, V. *Nature* **2000**, *407*, 340.
31. Grubbs, R. H.; Chang, S. *Tetrahedron* **1998**, *54*, 4413.
32. Grubbs, R. H.; Miller, S. J.; Fu, G. C. *Acc. Chem. Res.* **1995**, *28*, 446.
33. Ivin, K. J.; Mol, J. C. *Olefin Metathesis and Metathesis Polymerization*, 2nd Ed.; Academic Press: San Diego, 1997.
34. Trnka, T. M.; Grubbs, R. H. *Acc. Chem. Res.* **2001**, *34*, 18.
35. Fürstner, A. *Angew. Chem., Int. Ed. Engl.* **2000**, *39*, 3012.
36. Nicolaou, K. C.; Winssinger, N.; Pastro, J.; Ninkovic, S.; Sarabia, F.; He, Y.; Vourloumis, D.; Yang, Z.; Li, T.; Giannakakou, P.; Hamel, E. *Nature* **1997**, *387*, 268.
37. Hermann, T.; Westhof, E. *J. Mol. Biol.* **1998**, *276*, 903.
38. Hermann, T.; Westhof, E. *J. Med. Chem.* **1999**, *42*, 1250.
39. National Committee for Clinical Laboratory Standards. In Approved Standard M7-A5: Methods for Dilution Antimicrobial Susceptibility Tests for Bacteria That Grow Aerobically, 5th Edition (Wayne, PA: National Committee for Clinical Laboratory Standards). **2000**, *327*, 389–394.
40. de Lencastre, H.; Cuoto, I.; Santos, I.; Melo-Cristino, J.; Torres-Pereira, A.; Tomasz, A. *Eur. J. Clin. Microbiol. Infect. Dis.* **1994**, *13*, 64.
41. Sanches, I. S.; Ramirez, M.; Troni, H.; Abecassis, M.; Padua, M.; Tomasz, A.; de Lencastre, H. *J. Clin. Microbiol.* **1995**, *33*, 1243.
42. Scudiero, D. A.; Shoemaker, R. H.; Paull, K. D.; Monks, A.; Tierney, S.; Nofziger, T. H.; Currens, M. J.; Seniff, D.; Boyd, M. R. *Cancer. Res.* **1988**, *48*, 4827.